MASTER THESIS

Assessing Single and Dual-Sensor IMU Setup for 3D Foot Modelling in Running

Miriam Ghiani

FACULTY OF ELECTRICAL ENGINEERING,
MATHEMATICS AND COMPUTER SCIENCE

BIOMEDICAL SIGNALS AND SYSTEMS (BSS)
RESEARCH GROUP

EXAMINATION COMMITTEE
dr. Jasper Reenalda
dr.ir. Frank J. Wouda
dr.ir. Mohamed Irfan Refai

8 April 2025

UNIVERSITY OF TWENTE.

ABSTRACT

Background: Accurate measurement of foot kinematics is essential for gait analysis, injury prevention, and performance assessment. While optical motion capture (OMC) remains the gold standard for multi-segment foot modelling, inertial measurement units (IMUs) offer a portable and inexpensive alternative. However, most IMU-based approaches rely on a single foot-mounted sensor, treating the foot as one rigid segment and neglecting independent foot segment motion. **Objective:** This study investigates the accuracy of a dual-sensor IMU setup compared to a single-sensor IMU setup for estimating hindfoot–forefoot (HF/FF) joint angles using a multi-segment foot model during running. Accuracy is evaluated relative to optical motion capture (OMC) as the reference standard and with additional focus on the influence of running speed and foot strike pattern, forefoot striker (FFS) vs. rearfoot striker (RFS). **Methods:** Six healthy recreational runners (3 rearfoot strikers, 3 forefoot strikers) ran on an instrumented treadmill at two speeds (9 and 11 kph), while foot segment orientations were recorded using inertial measurement units (IMUs) and optical motion capture (OMC). A dual-IMU setup captured hindfoot and forefoot orientation directly, while a single-IMU setup estimated forefoot orientation from the hindfoot. HF/FF joint angles from both IMU setups were compared to OMC using root mean square error (RMSE) and standard deviation (SD) across the gait cycle, both overall and separately by strike pattern. Additionally, per-subject error mean and SD, as well as correlation values between the IMU setups and the OMC, were calculated. **Results:** Both IMU setups show similar overall error patterns, with the largest differences around toe-off. The dual-IMU setup showed improved accuracy during push-off, but slightly higher variability across the other phases. RMSE and SD increased at the higher speed (11 kph). Correlation with OMC was generally higher for the dual-IMU setup, yet no consistent differences in mean error were observed between the two IMU configurations. While running speed affected both setups similarly, by increasing error and lowering correlation, the strike pattern had minimal effect on performance. **Conclusion:** Given the added complexity of dual-sensor configurations, single-IMU setups may be sufficient for general gait analysis, whereas the dual-IMU setup may be preferable for applications requiring detailed forefoot motion tracking or improved accuracy during dynamic push-off phases.

INTRODUCTION

Running is a worldwide practised activity, both recreationally and professionally, serving as the foundation for many sports. Its accessibility and habitual incorporation into daily life offer significant health benefits [1]. However, it is associated with a high risk of running-related injuries, particularly in the lower extremities [2]. To improve injury prevention and performance analysis, accurate assessment of biomechanical risk factors is crucial. Despite extensive research, accurately analysing running biomechanics to predict injury risks remains challenging due to methodological limitations, variability in research approaches, and the complexity of human movement [3, 4]. This calls for an objective tool to assess gait parameters and lower extremity kinematics.

Instrumented gait analysis provides a systematic approach for studying human movement, with marker-based motion capture widely considered the gold standard for capturing high-accuracy kinematics [5, 6]. Optical motion capture (OMC) systems allow for detailed multi-segmental marker tracking and have been extensively used in quantitative gait analysis, providing valuable insights into three-dimensional foot segment kinematics for clinical in-vivo applications [7, 8]. However, their applicability outside of controlled laboratory settings is limited, as they rely on fixed camera setups that confine the measurement space. Additionally, OMC data processing is both computationally demanding and labour-intensive, requiring extensive post-processing of marker trajectories.

To overcome these constraints, inertial measurement units (IMUs) have gained increasing attention as a small, portable, and cost-efficient alternative to OMC [9], enabling motion analysis beyond laboratory settings. They measure acceleration and angular velocity and often include a magnetometer for heading estimation. This data can be used to estimate segment orientations and joint angles [10]. IMUs have been used in gait assessments for over a decade, initially focusing on basic kinematic parameters such as segment orientation, angular velocity, and acceleration, particularly for the ankle and foot [11, 12]. More recent research has explored their potential to measure spatiotemporal parameters in running, like foot strike and toe-off events with improved accuracy to estimate stride time, ground contact time and flight phase [13].

IMUs are now widely applied in running gait analysis to capture lower limb joint kinematics, detect gait events, and assess movement patterns [14]. Studies suggest that IMUs are a reliable tool for capturing lower-limb kinematics, demonstrating good validity in joint angle calculation compared to OMC systems [15, 16]. Additionally, IMUs have been applied for broader gait assessments, including identifying foot strike patterns, ground contact time, and pronation severity, aiding in biomechanical evaluations for injury prevention and footwear selection [17]. Their ability to provide gait analysis in real-world and low-resource settings makes them a practical alternative to laboratory-based motion capture systems.

However, most IMU-based gait analyses rely on collecting movement data with a single foot-mounted IMU placed on the dorsum, treating the foot as one rigid segment and neglecting its multi-segmental motion [17, 18, 19]. Studies using multi-segment foot models in OMC have shown that this simplification limits the accuracy of foot angle estimation and fails to capture the independent motion of the hindfoot (HF) and forefoot (FF) [20, 21]. Accurately capturing the independent movement of these segments is essential for calculating the joint angle between them, leading to a more precise representation of dynamic foot mechanics during running. OMC-based multi-segment models, e.g. the Leardini model [22] or the Oxford model [23], have been well established for detailed biomechanics analysis and are frequently used for precise assessment of foot kinematics [7].

Despite their widespread use in OMC, multi-segment IMU models remain limited. This is because a single IMU can only capture the motion of the segment to which it is attached, requiring multiple IMUs on the foot to achieve multi-segment motion analysis. This approach is less practical than the flexible marker-based method, often leading to the foot being treated as a rigid segment. The simplification of the foot as a single rigid segment not only limits joint angle estimation but also affects the accuracy of IMU-based centre of pressure (CoP) estimation, reducing the precision of inverse dynamics that rely on accurately capturing force distribution and load shifts between foot segments [24, 25].

One recent study measured foot movement using three foot-mounted IMUs and one on the shank [26], while another employed the same setup but with in-house built sensors [27]. While these approaches concentrate exclusively on foot kinematics, more recent research has implemented a dual IMU sensor setup within a full lower body measurement system (9 IMUs in total) to propose [28] and validate [29] a multi-segment model for gait analysis. However, all of these studies focus exclusively on walking, where movement amplitudes and impact forces are lower than during running, which, in contrast, introduces higher variability in lower limb kinematics and a greater range of motion of joint angles. Additionally, previous work has shown that higher running speeds can affect IMU measurement accuracy due to increased segment acceleration, leading to greater signal drift and estimation bias, particularly in joint angle or temporal parameter estimation [30, 19]. Different strike patterns alter segmental orientation, leading to distinct foot joint rotations and segment interactions, which cannot be captured by a single-segment foot model [31, 32]. This requires greater adaptability to manage its complex and dynamic conditions [33] which further underscores the need to explore multi-segment IMU models.

Despite the increasing use of IMUs in gait analysis, the comparison between single and dual-sensor setups for accurate 3D foot modelling remains unexplored. Existing studies primarily aim to identify running gait outcomes or examine the effects of factors such as injury, fatigue, individual characteristics, or footwear on gait, rather than focusing on detailed foot segment interactions [9].

This study aims to compare two IMU-based approaches for modelling foot segment motion: a **dual-sensor setup**, where both hindfoot and forefoot orientations are directly measured, and a **single-sensor setup**, where forefoot (FF) orientation is estimated from the hindfoot (HF) orientation. Rather than comparing single- vs. multi-segment models, as done previously [28], this study evaluates whether a dual-sensor setup improves joint angle estimation at the ball of the foot joint, defined here as the hindfoot–forefoot (HF/FF) joint. By assessing the accuracy, the study examines the trade-offs and practical usability of a dual-sensor setup in applied settings. While a dual-sensor setup may enhance foot motion representation, it also introduces increased setup complexity, sensor attachment requirements, and potential runner discomfort. The study aims to determine whether the accuracy benefits of an additional IMU justify these practical challenges in real-world applications, and could potentially contribute to advancements in IMU-based CoP estimation methods.

To achieve these aims, the study will analyse joint angle errors across both setups to assess whether a two-sensor approach enhances foot orientation representation, particularly under varying conditions such as different foot strike patterns and two running speeds. The accuracy of both approaches will be quantified by comparing joint angles derived from single- and dual-IMU sensor-based data to those obtained from the OMC reference system.

METHODS AND MATERIALS

This study was part of a larger research project that included an extended data collection protocol, but only parts related to this research were included.

Participants

Six healthy recreational runners (male-to-female ratio: 3:3; age: 26.5 ± 4.1 years; height: 184.5 ± 8.6 cm; weight: 76.0 ± 10.6 kg) participated in this study. The group consisted of 3 rearfoot strikers (RFS) and 3 forefoot strikers (FFS), with an average of 12.0 ± 7.5 years of running experience. Participants reported running 110.8 ± 84.2 km per month over 12.2 ± 6.1 sessions.

Participants were recruited from local running associations and student groups. All had no major injuries in the past six months and were experienced with treadmill running. They were able to sustain a running speed of 13 kph (3.61 m/s) for at least 5 minutes and were selected based on running at least 20 km per week. Strike patterns were assessed prior to the trials with a slow-motion video recording of the foot while running a short distance. Participants were categorized as forefoot strikers or rearfoot strikers based on whether the forefoot or heel made initial contact with the ground. If either strike pattern was clearly identifiable, the participant was invited to the measurements.

The experimental protocol was approved by the local ethics committee (University of Twente, Computer & Information Science; Reference no.: 240073). All participants provided informed verbal and written consent after receiving detailed information about the study.

Seven participants initially volunteered for the study. However, one participant was excluded due to a malfunction of the IMU setup during measurements.

Setup and Data Collection

The study was conducted in the Biomechanics research lab at the University of Twente, where kinematic and kinetic data were collected using inertial measurement units (IMUs), an optical motion capture (OMC) system, and an instrumented treadmill.

Participants were equipped with the Xsens MVN Link system (Movella Technologies BV, Enschede, the Netherlands), consisting of eight IMUs sampling at 240 Hz. The IMUs were placed according to the manufacturer's guidelines on the shank, thigh, pelvis, and sternum (Fig. 2). Additionally, one forefoot IMU per foot was mounted on a metal fixture attached to neutral running shoes shown in Fig. 1, making it a total of 10 IMUs. All IMUs were attached to the body using skin-friendly double-sided tape and additional tape atop the sensor. To further minimize motion artefacts, the lower leg IMUs were reinforced with compression socks, as proposed by Scheltinga et al. [18].

Figure 1. Provided neutral running shoe with metal fixture for the forefoot IMU and screws to fixate the lateral optical markers on the foot.

Fifty reflective markers were attached to the participants. These markers were tracked by an optical motion capture system (Qualysis AB, Gothenburg, Sweden) using eight optical cameras and two additional video cameras. The system operates at a sampling frequency of 128 Hz. The foot marker setup was based on the Leardini model [22] but was modified to fit a two-segment foot model of fore- and hindfoot, instead of three segments. Only two markers on the midfoot were excluded from the original setup, leaving overall more markers per segment. This adjustment was made to account for potential marker loss during running, particularly on the medial side of the foot, which can occur due to collisions or contact during movement. The lateral markers were held in place by screws in the provided shoe to minimize the risk of loss in that area. The toe markers, LFM, LFL (left) and RFM and RFL (right) (Fig. 2, C, D), were repositioned onto the screws on top to accommodate the metal fixture holding the additional forefoot IMU, which occupied space in the same region. The fixture provided two stable points for secure marker placement. Participants also wore pressure insoles (Moticon OpenGo 3.12.1, Moticon GmbH, Munich, Germany) inside their shoes during all trials. The data recorded by the insoles was not included in this analysis, as they were part of a separate study.

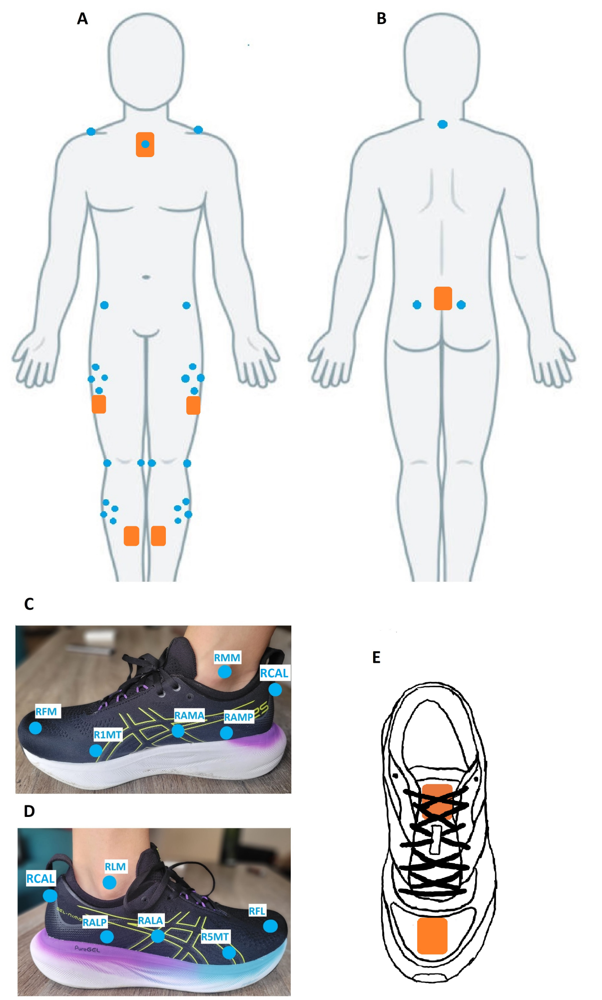

Figure 2. Optical marker (blue) and IMU (orange) placement on (**A**) the front of the body and (**B**) the back of the body. (**C**) The optical marker placement on the inside and (**D**) the outside of the right foot. (**E**) The top view of the foot shows the IMU placement.

Protocol

Running trials were conducted on one belt of a split-belt instrumented treadmill (Bertec Fit 5, Bertec Corporation, Columbus, OH, USA) with integrated force plates sampling at 1000 Hz. Participants completed 300-meter trials at two speeds, 9 kph and 11 kph (2.5m/s and 3.1m/s). Between trials, participants rested for 2 minutes to mitigate fatigue. Three vertical jumps were performed by participants on the treadmill before and after each running trial. They were executed after all measurement systems were turned on and served as reference points for time synchronization later. Calibration of all devices was performed according to the manufacturer's guidelines before each session.

Data processing

MT Manager (Xsens MT Manager; version 2022.0.0) was used to acquire the raw quaternion data representing the IMU orientations. OMC trajectory data was labelled and extracted using Qualysis Track Manager (QTM, Qualysis AB, Gothenburg, Sweden; version 2023.3). Force plate data were also exported through the motion capture software QTM. MATLAB (MathWorks Inc.; version 2021b) was used for all subsequent data processing.

An overview of the full data processing pipeline is provided in Fig. 4, including preprocessing, sensor orientation calculation, and the sensor-to-segment alignment steps. The following sections describe each of these steps in detail.

Sampling and Time Synchronization

Marker trajectories from the OMC system, vertical ground reaction forces (vGRF) from the force plates and sensor orientation for the IMUs were all resampled to a common sampling frequency of 200 Hz to ensure consistency across systems. Resampling was performed using MATLAB, applying a low-pass filter and interpolation to change the sampling rate while minimizing the risk of introducing artefacts.

The OMC system and treadmill force plates were inherently synchronized during recording, while they needed to be time-aligned with the IMU data. This was achieved using cross-correlation and a lag correction procedure based on the vertical jumps measured at the start of each trial, as described in the section *Protocol*. The timing of the measurement start of the systems was not consistent throughout the trials. The lag was therefore applied to the system data that started earlier, shifting it to align with the data that started later. After alignment, the longer dataset was trimmed to match the length of the shorter dataset. Once aligned, all data had consistent length, sampling rate, and timing.

Reference Coordinate System Alignment

To accurately compare sensor orientations and joint angles between the IMU and OMC systems, it is necessary to express these parameters in a common reference frame. Both systems define segment orientations relative to their respective local coordinate systems (CS), which differ in their axis definitions, as shown in Fig. 3.

The IMU system followed a right-handed coordinate system (x-axis pointing forward, y-axis to the left, and z-axis upward). In contrast, the OMC system's local coordinate system had the z-axis pointing to the right and the y-axis pointing upward.

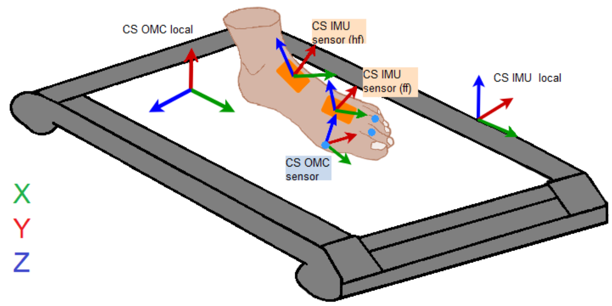

Figure 3. Visualization of local OMC and IMU reference system, as well as sensor-fixed coordinate systems (CS) for fore- and hindfoot of the IMUs (orange) and forefoot of the optical markers (light blue).

The rotation matrices representing the local IMU coordinate systems were as follows:

$$\mathbf{R}_{\text{local,OMC}} = \begin{bmatrix} 1 & 0 & 0 \\ 0 & 0 & 1 \\ 0 & -1 & 0 \end{bmatrix}, \quad \mathbf{R}_{\text{local,IMU}} = \begin{bmatrix} 1 & 0 & 0 \\ 0 & 1 & 0 \\ 0 & 0 & 1 \end{bmatrix}.$$

Due to these differences, segment orientations calculated for both systems cannot be directly compared. To unify the reference frame, the OMC coordinate system was transformed by rotating all marker trajectories $-90°$ around the x-axis. The transformation rotation matrix for this alignment was computed as:

$$\mathbf{R}_{\text{transCS}} = \begin{bmatrix} 1 & 0 & 0 \\ 0 & \cos(-90°) & -\sin(-90°) \\ 0 & \sin(-90°) & \cos(-90°) \end{bmatrix} = \begin{bmatrix} 1 & 0 & 0 \\ 0 & 0 & -1 \\ 0 & 1 & 0 \end{bmatrix}$$

The locally aligned marker trajectories were computed by applying the transformation shown in Eq. 2. The trajectory data expressed in the local reference frame of the OMC ($\mathbf{R}_{\text{source}}$) is multiplied with the transformation matrix $\mathbf{R}_{\text{transCS}}$ expressed as $\mathbf{R}_{\text{trans}}$ to obtain $\mathbf{R}_{\text{aligned}}$, the trajectory data expressed in the local reference frame of the IMU system. By applying this, all orientations and joint angles that will be derived from both systems can now be expressed within the same local coordinate system.

Sensor Orientation

Forefoot and hindfoot segments for both feet, as well as the pelvis segment, were defined using marker trajectories from the OMC system (Fig. 5). The orientations rotation matrices were computed using the Triad method, from three non-collinear markers and cross-product calculations, as described in literature [34].

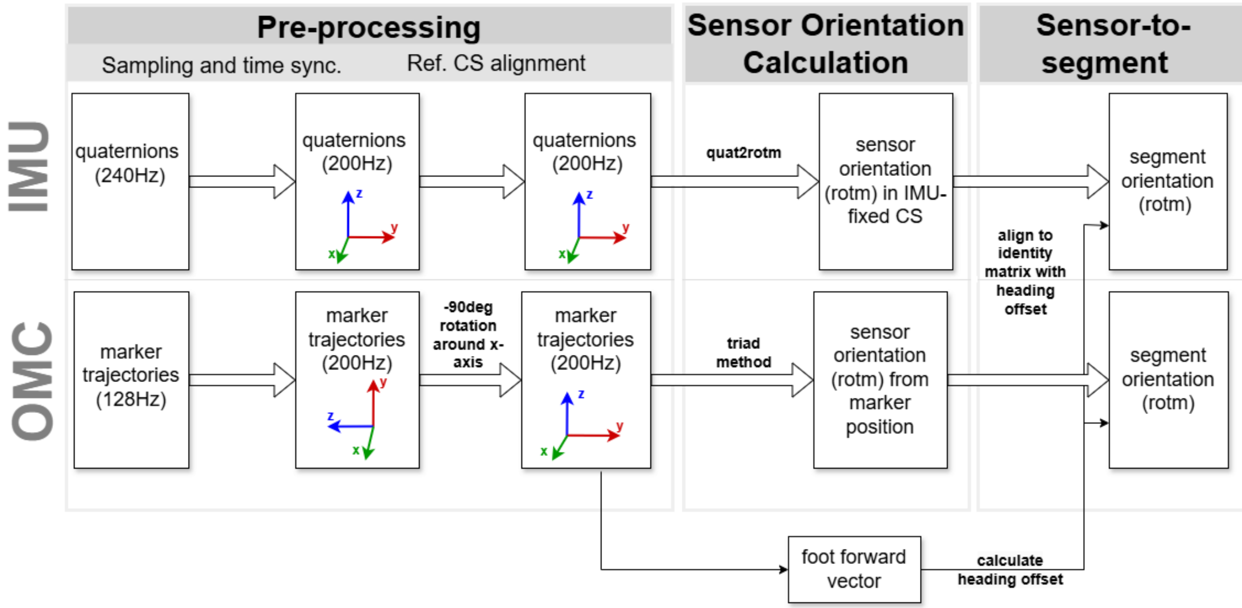

Figure 4. Overview of the full data processing pipeline from measured IMU and OMC input to segment orientation. The coordinate systems shown represent the local reference frames (system-fixed) to visualise rotations into a common reference frame. The steps shown here are described in detail in the corresponding sections of this study.

The x-axis was defined from the back to the front, the y-axis from the right to the left, and the z-axis as the cross-product between the x-axis and y-axis, to express them similar to the direction of the local right-handed reference system. To ensure perpendicularity, the x-axis was recalculated afterwards by taking the cross-product between y- and z-axis. The rotation matrix for each segment in the local CS of the OMC was then constructed.

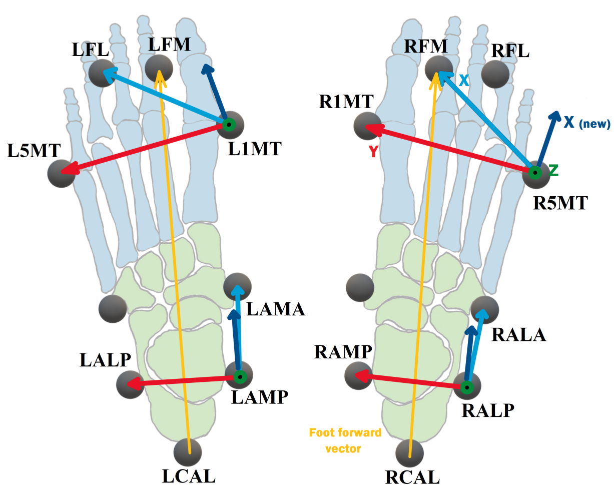

Figure 5. Marker trajectories used for segment orientation creation using the Triad method. The initial X-axis is represented by the light-blue vector, the y-axis by the red vector, and the z-axis by the green vector (pointing upwards). The recalculated x-axis is shown in dark blue. The vector describing the forward direction of the foot is shown in yellow.

These orientations effectively represent the sensor orientations within the local reference system, as they depend on marker placement, similar to how IMU sensor orientations depend on sensor placement. For the OMC-based method segment orientations are computed using marker trajectories, while the IMU system records quaternions describing the orientation of the sensor-fixed coordinate system. However, in both cases, the resulting sensor orientation rotation matrices are not inherently aligned with the anatomical foot segments (see Fig. 6, requiring an additional sensor-to-segment alignment step (see Section *Sensor-to-Segment Alignment*). The difference in their respective sensor-fixed coordinate systems is illustrated in Fig. 3.

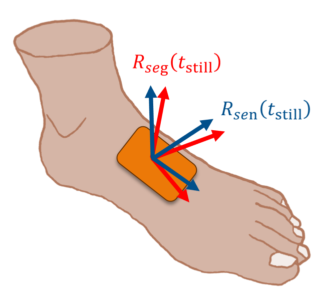

Figure 6. Difference in sensor orientation (blue) and segment orientation (red) before alignment. On the example of the IMU on the hindfoot.

Sensor-to-Segment Alignment

To align the sensor orientation with the anatomical segment orientation, a transformation rotation matrix $\mathbf{R}_{\mathrm{trans}}$

is computed at a frame where the subject is standing still. This static posture-based alignment is also used in the Xsens MVN model for sensor-to-segment calibration [35]. The transformation is done from both sensor orientations, based on the marker and IMU data, to the orientation of the same segment.

In general, the transformation rotation matrix is computed as:

$$\mathbf{R}_{\text{trans}} = \mathbf{R}_{\text{target}}(t_{\text{still}})\mathbf{R}_{\text{source}}^{\top}(t_{\text{still}}) \tag{1}$$

where:

- $\mathbf{R}_{\text{source}}(t_{\text{still}}) \in \mathbb{R}^{3\times 3}$ is the orientation rotation matrix to be transformed at the still-standing frame,
- $\mathbf{R}_{\text{target}}(t_{\text{still}}) \in \mathbb{R}^{3\times 3}$ is the target orientation rotation matrix at the still-standing frame,
- $\mathbf{R}_{\text{source}}^{\top}(t_{\text{still}})$ is the transpose of $\mathbf{R}_{\text{source}}(t_{\text{still}})$.

Once $\mathbf{R}_{\text{trans}}$ is computed, it is applied to all frames of the orientation data to transform. The aligned rotation matrices for each time step are computed as:

$$\mathbf{R}_{\text{aligned}}(t) = \mathbf{R}_{\text{trans}}\mathbf{R}_{\text{source}}(t) \tag{2}$$

where:

- $\mathbf{R}_{\text{source}}(t) \in \mathbb{R}^{N\times 3\times 3}$ is the orientation rotation matrix to be transformed at each time step t,
- $\mathbf{R}_{\text{aligned}}(t) \in \mathbb{R}^{N\times 3\times 3}$ is the target orientation rotation matrix at each time step t.

$\mathbf{R}_{\text{aligned}}(t)$ expresses the anatomical segment orientation in the local coordinate system. Since the transformation matrix $\mathbf{R}_{\text{trans}}$ is constant and computed only once per measurement system, from the still-standing frame, it is applied uniformly across all frames to ensure the sensor orientations are consistently aligned with the segment orientations.

During the still standing, it is assumed that the foot is flat on the ground, meaning that its segment orientation should align with the global reference frame. This allows the segment orientation at this frame to be approximated as the identity matrix, which represents perfect alignment with the right-handed coordinate system. However, there is a heading offset, as the foot is not necessarily pointing in a perfect forward direction. This offset is accounted for by determining the foot's forward-facing direction using the foot forward vector. It is calculated using the trajectories of the heel and medial toe marker, visualized in Fig. 5. By incorporating this heading adjustment, the transformation ensures that the segment orientations are properly expressed and are the same for the IMU- and OMC-based approach.

Gait Event Detection

Gait events were identified using vertical ground reaction force (vGRF) data recorded from the treadmill force plates. The vGRF signal was filtered, using a 4th-order Butterworth low-pass filter, with a cut-off frequency of 20 Hz to remove high-frequency noise. A threshold of 35 N was applied to the data to detect initial contact (force crossing the threshold from below) and toe-off (force crossing the threshold from above). This threshold was chosen based on literature values, which typically range from 20 N [36] to 50 N [37], as well as the specific characteristics of the treadmill and the data collected in this study. The events detected were primarily used for forefoot orientation estimation by determining phases of ground contact and air time.

Additionally, the detected initial contact events were later used in stride segmentation of the joint angle for error calculation, where the data was divided into individual strides and interpolated to a standardized length of 200 frames.

Forefoot Orientation Estimation

Since this study compares a single-sensor vs. dual-sensor setup using a multi-segment foot model, estimating forefoot orientation is necessary to enable joint angle calculations when only one IMU is available, i.e. in the single-IMU sensor setup. In a dual-sensor setup, both the hindfoot and forefoot orientations are directly measured, allowing for direct computation of the joint angle between the two segments. However, in a single-sensor setup, only the hindfoot orientation is recorded, requiring the forefoot orientation to be estimated. This estimation was based on the orientation data of the hindfoot sensor. To segment the gait cycle, the identified initial contact and toe-off events (see section *Gait Event Detection*) are used to identify the contact and flight phase.

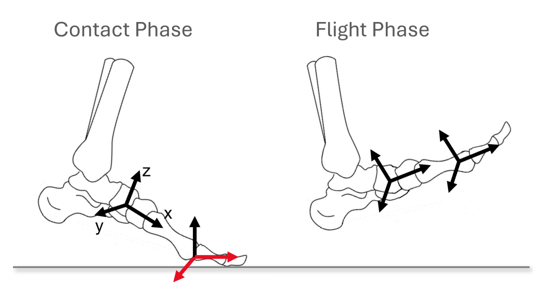

Figure 7. Estimated forefoot orientation during contact and flight phases. In flight, the forefoot follows the hindfoot orientation (black). In contact, the forefoot is assumed flat in x-y-plane (red), except for the heading direction, which follows the hindfoot (black). Figure adapted from [31].

During the flight phase (between toe-off and initial contact), the forefoot orientation was assumed to be identical to the measured hindfoot orientation. In the stance phase, when ground contact was detected, the forefoot was set to a flat orientation, aligning with the identity matrix but with the heading offset taken from the hindfoot orientation rotation matrix at still standing (Fig. 7). The orientation of the measured hindfoot and estimated forefoot orientation over one stride is shown in Fig. 8.

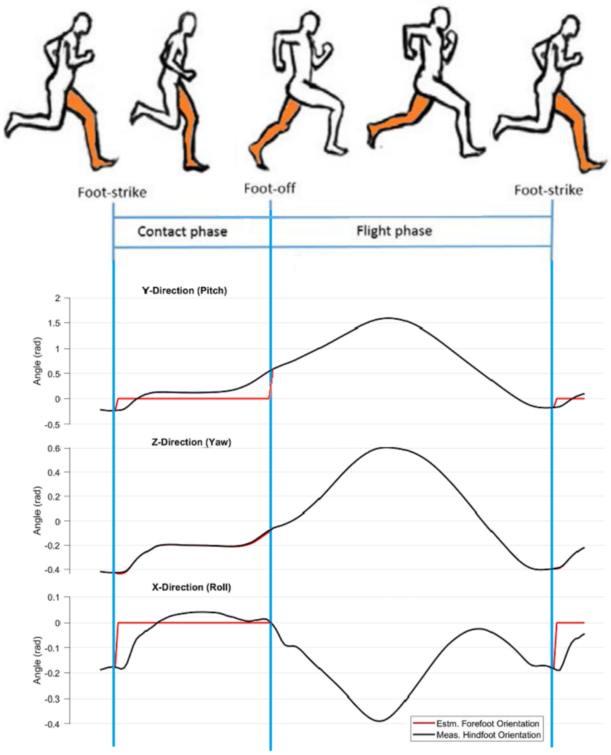

Figure 8. Visualization of the forefoot orientation estimation method over one stride, aligned with the gait cycle and its key gait events, for a rearfoot striker. The upper part of the figure illustrates the running gait phases, adapted from [13], with modifications to scaling, titles, and the addition of orientation graphs below.

Joint Angle Calculation

To quantify the error between the OMC and the IMU setups, the joint angles were computed by deriving the relative transformation rotation matrix between the hindfoot and forefoot orientations within the same foot and measurement system (IMU and OMC), as shown in Eq. 1.

Additionally, this calculation was performed between the IMU-based measured hindfoot orientation and the estimated forefoot orientation to assess the feasibility of using a single IMU on the foot for HF/FF joint angle estimation. By comparing these joint angles, the error introduced by estimating the forefoot orientation instead of directly measuring it can be determined. The resulting joint angle data was cut in strides based on the foot-strike events detected earlier.

Outlier rejection

For the joint angle stride data obtained from the OMC system, outliers were identified using the interquartile range (IQR) method with upper and lower boundaries set at 10. This was used to detect and reject strides affected by marker switching in the Qualysis software. Given the natural variability in running and individual stride differences, the rejection boundaries were not chosen to be overly strict.

For the joint angle stride data obtained from the OMC system, outliers were identified using the interquartile range (IQR) method with upper and lower boundaries set at 10. This approach was used to detect and reject strides affected by marker switching in the Qualysis software while maintaining natural stride variability during running.

Additionally, to ensure comparability between feet, the heading direction (Z-direction) of joint angles in the left foot was inverted to match the right foot. Due to differences in the local coordinate system definition of each foot, the Z-axis in the left foot is opposite to the right foot, resulting in mirrored joint angle calculations between the forefoot and hindfoot. Without this adjustment, joint angles on the left foot would be inverted relative to the right, making direct comparison inconsistent [34].

Error Calculation and Analysis

To assess the accuracy of the IMU-based joint angles, the root mean square error (RMSE) was calculated for all valid strides by comparing them to the OMC reference. RMSE was computed separately for joint angles derived from the single-IMU setup and from the dual-IMU setup, each compared against the corresponding OMC joint angles. RMSE calculations were performed independently for joint angle movements around the three anatomical axes: Y (dorsiflexion/plantarflexion), X (inversion/eversion) and Z (internal/external rotation). From this point onwards, these axis-based movements will be referred to either by their anatomical movements or by the corresponding anatomical planes (Fig. 9).

A stride was considered valid if it was not rejected as an outlier in any of the stride datasets (OMC, dual IMU, or single IMU). Valid strides were aggregated across multiple participants, and both feet were included in the same error calculation. The two running speeds were processed separately due to timing differences in gait events. At higher speeds, the flight phase is longer, leading to earlier initial contact and toe-off events. For analyses focusing only on forefoot or rearfoot strikers, strides were further grouped based on participants exhibiting these strike patterns.

Given the small sample size (n=6), standard statistical analyses were constrained by low statistical power, limiting the robustness and generalizability of potential findings. Initially, tests for normality (Shapiro-Wilk) were conducted on the calculated mean errors for both IMU setups, confirming that the data were not normally distributed. Consequently, non-parametric tests such as the Wilcoxon signed-rank test and the Mann-Whitney U test were performed to assess differences between setups (single- vs. dual-IMU), speeds (9 kph vs. 11 kph), and strike pat-

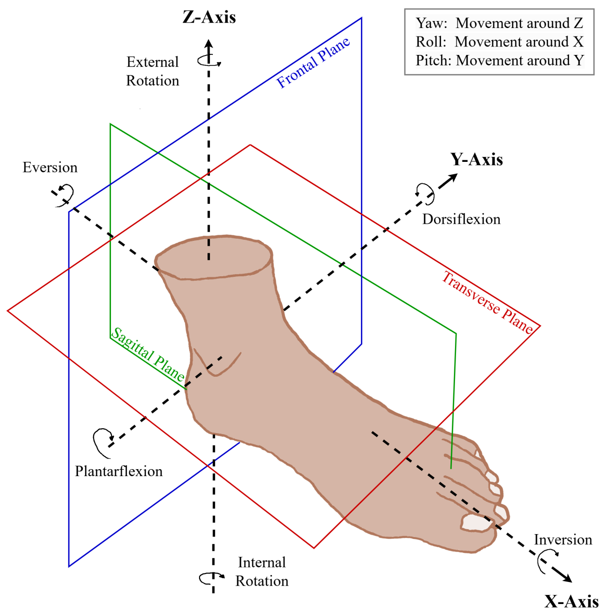

Figure 9. Overview of the axes, anatomical planes, and corresponding foot movements. Positive rotation directions follow the right-hand rule. Yaw, Roll, and Pitch denote rotations around the Z-, X-, and Y-axes respectively. The Z-direction is also referred to as heading direction.

terns (RFS vs. FFS). These tests yielded no statistically significant differences, likely due to the limited sample size and substantial variability within subjects. Statistical power was thus insufficient to reliably detect subtle yet practically meaningful differences under these conditions, especially with only six participants and two speeds. Considering these factors, the results presented here are better understood as descriptive rather than definitive.

Therefore, rather than relying solely on statistical significance testing, this study adopted a more descriptive approach. For a detailed comparison between the two IMU setups, summary tables were created that report mean errors and standard deviations (SD) per participant, speed, and direction, averaged over all frames and strides. Additionally, correlation analyses between each IMU setup and the optical motion capture reference were performed for each participant and speed to assess the strength and consistency of the linear relationship. Higher correlation values indicate stronger agreement between IMU-derived joint angles and the OMC reference, whereas lower correlations reflect greater discrepancies in error patterns. Therefore, correlation strength was categorized as *weak* ($q \leq 0.35$), *moderate* ($0.35 < q < 0.67$), *strong* ($0.67 \leq q < 0.90$), and *excellent* ($q \geq 0.90$) [38]. These descriptive analyses, complemented by detailed time-series graphs illustrating error trends throughout the gait cycle, provide context and practical insights into when and why differences in IMU accuracy occur.

RESULTS

Fig. 10 and Fig. 11 illustrate the absolute RMSE between IMU-based hindfoot-forefoot (HF/FF) joint angles and those obtained from the OMC system, which is considered the gold standard. The comparison includes both single-sensor and dual-sensor IMU setups. Across all conditions, both IMU setups exhibit similar overall trends in HF/FF joint angle errors, with magnitudes varying across planes and gait phases. The most prominent differences appear in the sagittal plane, particularly around toe-off ($\sim$30% gait cycle), where the single-IMU setup shows the highest error values and elevated variability. During mid-stance and swing phases, the single-IMU setup occasionally outperformed the dual-IMU in absolute error. In the transverse plane (heading), error levels remain more consistent throughout the gait cycle but exhibit a larger standard deviation, indicating higher variability across participants. In contrast, the frontal plane generally shows smaller errors across the gait cycle, with no distinct peaks as seen in the other axes. Comparing speeds, the 11 kph condition shows overall higher RMSE values than 9 kph, particularly in the sagittal plane.

When separating foot strike patterns (Fig. 11), error trends remain largely consistent between RFS and FFS. While FFS exhibit slightly higher peak errors around toe-off, the differences are subtle. RFS show a brief drop in error around 10% of the gait cycle compared to FFS. Across both groups, the highest errors occur in the late stance phase, followed by more stable error levels during midstance. As for Fig. 10, the RMSE and SD at 11 kph are higher than for 9 kph, for both strike patterns.

To further quantify these observations, Tab. 1 and Tab. 2 summarize the mean and standard deviation of the RMSE per participant, speed, and IMU setup. Additionally, the correlation between each IMU setup and the OMC system is provided, offering insight into the consistency of the measurements.

9 kph

Subject	**Error** [°]		**Correlation**	
	Dual IMU (Mean ± SD)	Single IMU (Mean ± SD)	Dual IMU vs. OMC	Single IMU vs. OMC
S1 (FFS)	6.88 ± 4.36	$\mathbf{5.25 \pm 6.58}$	**0.8**	0.7
S3 (RFS)	$\mathbf{2.00 \pm 1.55}$	4.63 ± 5.09	**0.84**	0.57
S4 (RFS)	17.23 ± 4.22	$\mathbf{8.21 \pm 9.16}$	**0.62**	0.54
S5 (RFS)	$\mathbf{3.38 \pm 2.68}$	5.03 ± 6.48	**0.7**	0.56
S6 (FFS)	6.92 ± 5.59	$\mathbf{6.15 \pm 6.53}$	**0.83**	0.75
S7 (FFS)	10.53 ± 3.12	$\mathbf{9.39 \pm 8.21}$	**0.85**	0.71

Table 1. Comparison of error in HF/FF joint angles between dual-IMU and single-IMU setups (compared to OMC as reference) for 9 kph on subject-level with strike pattern indicated as FFS (Forefoot Striker) and RFS (Rearfoot Striker)). Lower error and higher correlation are **marked**.

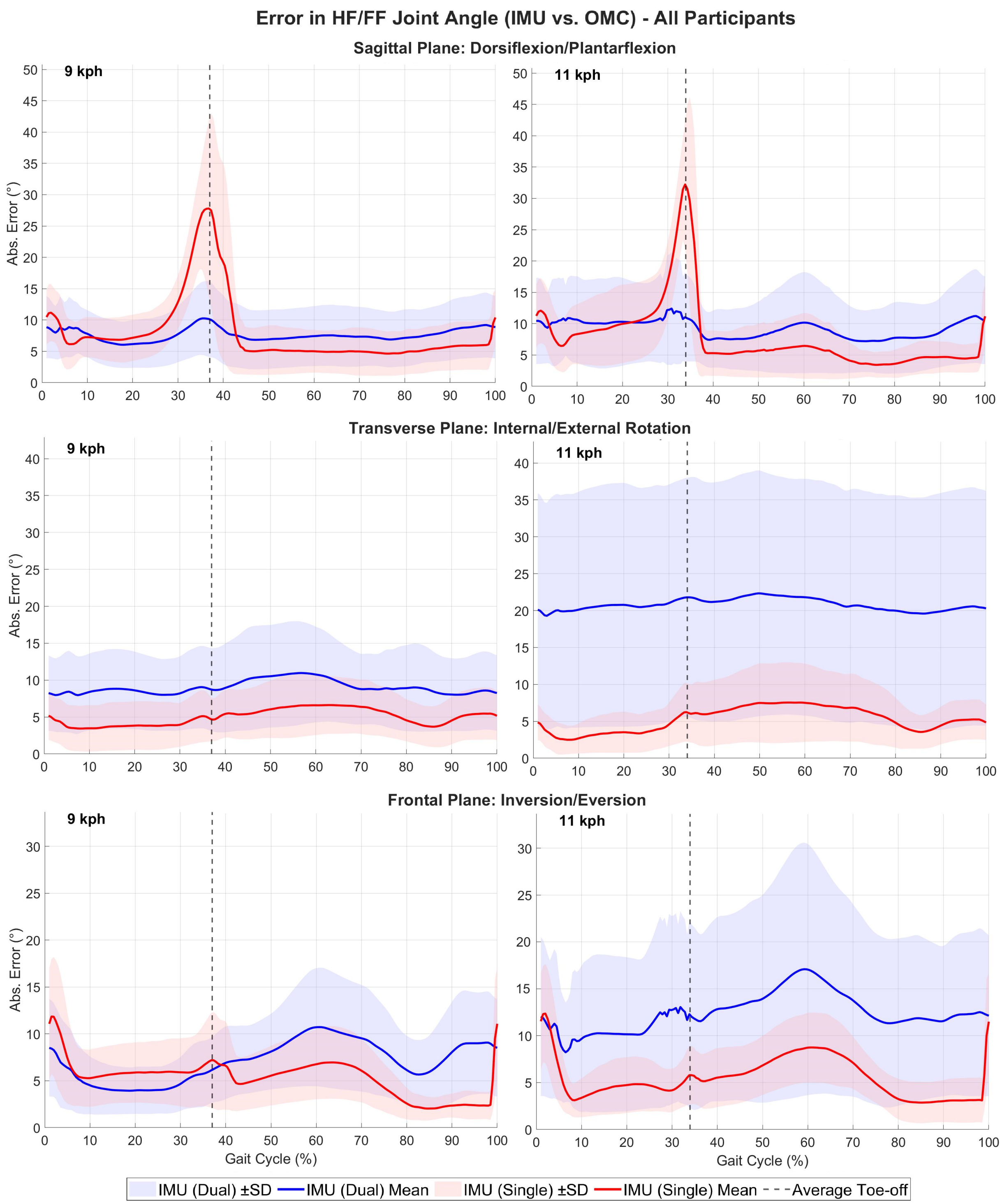

Figure 10. Error in HF/FF joint angles in the sagittal plane (dorsiflexion/plantarflexion), transverse plane (internal/external rotation), and frontal plane (inversion/eversion), between IMU and OMC systems for single and dual IMU-sensor setup, over all strike patterns.

Both IMU setups exhibit participant-dependent variations in error, with no consistent accuracy advantage observed for either setup across all subjects. The single-IMU setup generally shows higher variability, as indicated by larger standard deviations, compared to the dual-IMU setup, for both speeds.

At 11 kph, errors are generally higher than at 9 kph across both IMU setups, with the single-IMU setup displaying greater variability across speeds. Standard deviations tend to be larger at 11 kph, particularly for the

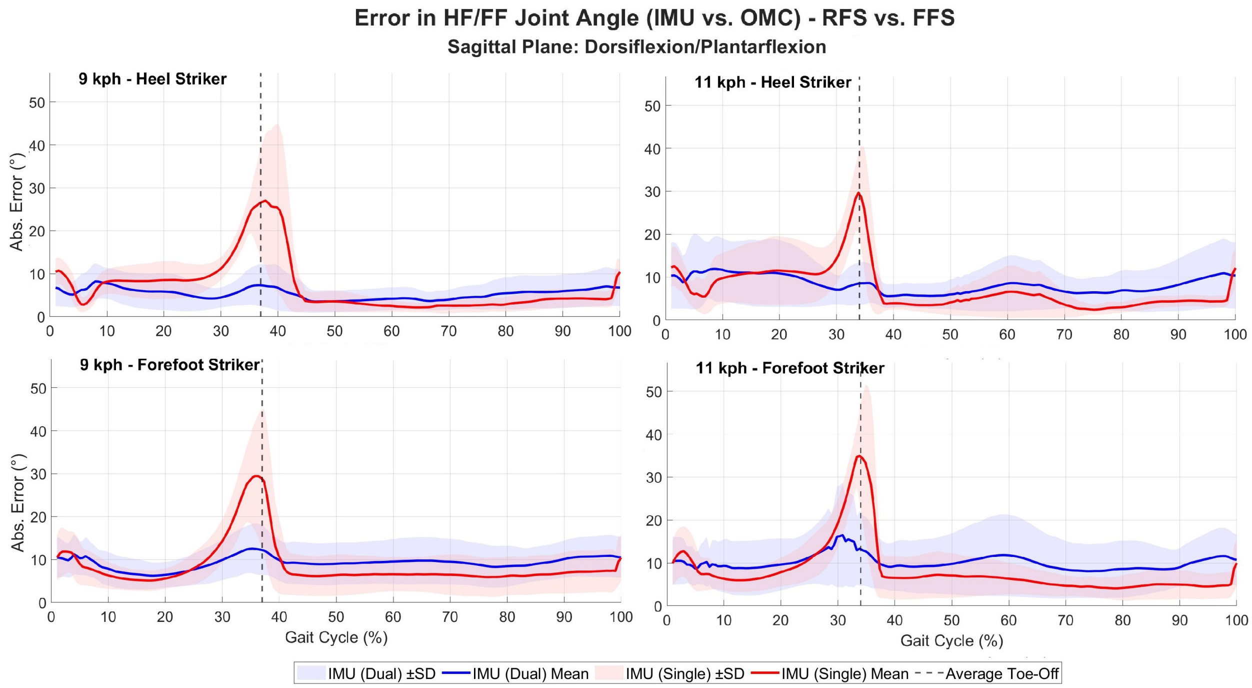

Figure 11. Error in HF/FF joint angles in the sagittal plane (dorsiflexion/plantarflexion) between IMU and OMC systems for single (red) and dual (blue) IMU-sensor setup, comparing heel-striker and forefoot-striker at two different speeds. The horizontal dotted line marks the average toe-off event per speed.

11 kph

Subject	Error [°]		Correlation	
	Dual IMU (Mean ± SD)	Single IMU (Mean ± SD)	Dual IMU vs. OMC	Single IMU vs. OMC
S1 (FFS)	9.50 ± 5.04	**5.94 ± 6.68**	**0.81**	0.68
S3 (RFS)	5.20 ± 3.31	**5.00 ± 4.85**	**0.75**	0.57
S4 (RFS)	10.98 ± 7.82	**7.70 ± 9.59**	**0.48**	0.38
S5 (RFS)	**3.10 ± 2.60**	4.86 ± 5.50	**0.77**	0.56
S6 (FFS)	**6.86 ± 9.82**	7.23 ± 7.22	0.67	**0.7**
S7 (FFS)	**5.82 ± 3.81**	7.14 ± 8.99	**0.83**	0.68

Table 2. Comparison of error in HF/FF joint angles between dual-IMU and single-IMU setups (compared to OMC as reference) for 11 kph, with strike pattern indicated as FFS (Forefoot Striker) and RFS (Rearfoot Striker). Lower error and higher correlation are **marked**.

single-IMU setup, indicating greater fluctuations in error.

Correlation values with the OMC system were typically higher for the dual-IMU setup. At 9 kph, five out of six participants showed *strong* to *excellent* correlations ($r > 0.67$) with the dual-IMU, while the single-IMU mostly remained in the *moderate* to *strong* range ($0.35 < r < 0.90$). At 11 kph, correlation strength decreased slightly for both setups, with a clearer drop for the single-IMU setup. In the dual-IMU setup, three participants dropped to *moderate* or *weak* correlation ($r \leq 0.67$), and the single-IMU showed only one *strong* correlation (S5), with most remaining *moderate* or lower.

When comparing values for foot strike patterns, both rearfoot strikers and forefoot strikers show similar error trends. There is no consistent advantage for either group in mean error, SD or correlation for either of the sensor configurations. Higher speed also affects both strike types similarly by lowering correlation and increasing mean error and SD.

DISCUSSION

This study compared single- and dual-IMU setups across multiple gait cycles to evaluate whether adding a second, forefoot-mounted sensor improves kinematic accuracy and whether such gains justify the added complexity in setup and handling.

Optical Motion Capture as the Reference System

To assess the plausibility of the OMC as a reference system, the forefoot–hindfoot joint angle in the sagittal plane (dorsiflexion/plantarflexion) was computed across 1688 strides at 9 kph and 1479 strides at 11 kph. The joint angle trajectories were illustrated across a normalized gait cycle, with standard deviations. The corresponding range of motion (ROM) was defined as the difference between the maximum and minimum HF/FF joint angle within the gait cycle.

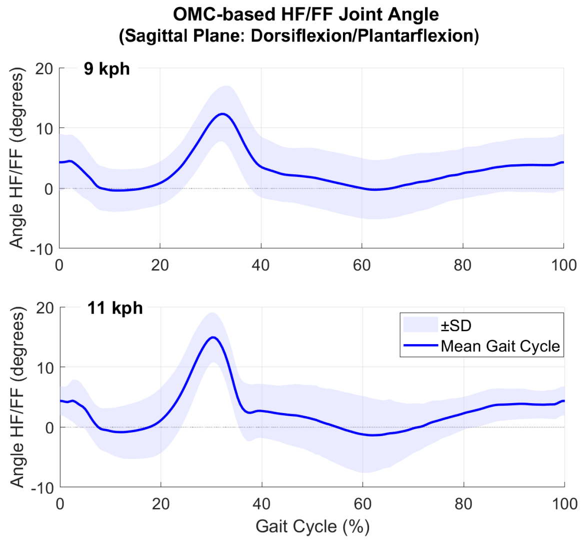

Figure 12. OMC-based HF/FF joint angle in sagittal plane across normalized gait cycles at 9 kph and 11 kph, including mean ± SD.

The resulting ROM values were $16.05° \pm 3.39°$ at 9 kph and $20.46° \pm 5.77°$ at 11 kph. These values align with previously published ROM of plantarflexion/dorsiflexion motion for the hindfoot–forefoot joint from multi-segment foot models using OMC. Schallig et al. [39] reported a ROM of $12.5° \pm 3.5°$, Wang et al. [40] reported $15.4° \pm 3.6°$, and Levinger et al. [41] reported 14.4°, all for walking. The slightly higher ROM observed in this study is expected, as running typically involves greater joint excursions than walking. Nevertheless, the similarity in ROM magnitude compared to walking studies still strongly supports the reliability of the current OMC reference data. The joint angle curves presented in Fig. 12 exhibit a dorsiflexion/plantarflexion motion pattern consistent with the general shape of forefoot–hindfoot interactions in the sagittal plane, reported in these prior studies. This further reinforces the plausibility and reliability of the reference system employed here.

Accuracy of Dual- vs. Single-Sensor Setup

The higher peak around the toe-off is likely due to the estimation approach for the single-IMU setup, which assumes the forefoot remains flat during stance and abruptly aligns it with the hindfoot in flight, creating a discontinuity in HF/FF joint angle estimation. Around toe-off, small stride-to-stride differences in push-off timing or foot posture may amplify these discontinuities, leading to the observed spike in standard deviation. This supports prior findings highlighting toe-off as a mechanically complex phase where simplifications in foot modelling can lead to inaccuracies [20]. While no temporal smoothing was applied to the estimated joint angles in this study, previous work suggests that filtering around dynamic transitions could help reduce such error spikes [42]. In contrast, the dual-IMU setup measures forefoot motion directly, enabling smoother transitions through toe-off and lower errors in this phase. Bauer et al. [29] similarly showed that adding a second IMU for a two-segment foot model in walking allowed for more detailed and phase-specific segment analysis and reported better repeatability, indicating *lower* variability, compared to a single-sensor setup. However, in the current study, the dual-IMU setup showed *higher* variability across the gait cycle, especially in phases where natural forefoot motion differs more strongly between strides. This inconsistency may be due to the inherently greater variability in foot segment motion during running compared to walking, which increases the likelihood of capturing stride-to-stride differences and movement artefacts with the additional forefoot sensor.

Angular differences in the frontal (inversion/eversion) and transverse (internal/external rotation) planes were either small or strongly affected by offset, making the sagittal plane (dorsiflexion/plantarflexion) the main focus. Previous studies have shown that during running, low motion amplitudes and high variability in these directions often reduce the accuracy of IMU-derived joint angles [32, 43, 44]. While those findings focus on the ankle or general foot segments, similar limitations are visible at the HF/FF joint in the current data. As shown in Fig. 10, errors in the frontal and transverse planes, especially in the dual-IMU setup, show large fluctuations over the gait cycle. Due to this reduced reliability, results in these axes were excluded from further analysis.

During mid-stance, the forefoot often aligns flat with the ground, which closely matches the estimation assumption and reduces HF/FF joint angle error, which could explain why the error of the single-IMU setup occasionally outperforms the dual-IMU. The same during swing, where the foot acts largely like a rigid segment with limited rotation around the metatarsal joint or other deformations, making the orientation estimation (i.e. equal to hindfoot) more valid [45]. Furthermore, IMU measurement quality is generally lower during swing compared to stance [16], potentially explaining the occasional advantage of the estimation-based method in this phase.

The RMSE and correlation values in Tabs. 1 and 2 offer a broader view of performance across participants and conditions. As expected, the dual-IMU setup achieves higher correlations, likely because it directly measures both the fore- and hindfoot segments, thereby closely aligning with the reference system. By contrast, the single-IMU relies on an estimation of the forefoot orientation, which can lower the correlation when a participant's actual motion deviates from the expected movement pattern. However, higher correlation in the dual-IMU setup did not consistently correspond to lower RMSE values compared to the single-IMU, indicating that individual gait characteristics strongly influenced accuracy outcomes. Although the mean standard deviation is typically higher in the single-sensor setup, this is largely driven by the error peak at toe-off, as variability per frame across most of the stride is lower compared to the dual-IMU (see Fig. 10). These modest accuracy improvements have also been reported in previous walking-based studies [29].

Impact of Running Speed on Accuracy

Increasing running speed from 9 kph to 11 kph consistently resulted in larger RMSE and higher variability (SD) in HF/FF joint angle errors for both the single- and dual-IMU setups. As shown in Fig. 10 (all participants) and Fig. 11 (RFS vs. FFS), the error curves become more pronounced at 11 kph. This pattern is also evident in Tabs. 1 and 2, where participants show higher mean errors, standard deviation and reduced correlation values at the faster speed.

At 11 kph, correlation values decreased for both IMU setups compared to 9 kph, with a clearer drop in the single-IMU setup. As shown previously, running introduces multi-planar motion and irregular velocities that reduce the validity of IMU-based measurements [30]. Similarly, lower correlations and higher RMSEs during running compared to walking have been reported in other studies [32, 46], and some have introduced speed-dependent correction strategies to address these effects [19]. The more pronounced drop in correlation for the single-IMU setup may reflect its reliance on estimated forefoot orientation rather than direct segment measurements. During dynamic phases like push-off and foot-strike, faster running introduces greater noise in the measured forefoot data due to impact artefacts or sensor movement [17]. While the dual-IMU setup and OMC both capture this noise at the forefoot, helping preserve waveform similarity, the single-IMU setup estimates forefoot motion from the hindfoot. As a result, the noise characteristics differ between systems, and slight timing mismatches can occur. These discrepancies can reduce alignment with the OMC reference and lower overall correlation.

While both IMU setups deteriorate in accuracy with speed, there is no clear advantage of one system over the other at 11 kph. The data indicate that single- and dual-sensor configurations are similarly affected by the faster, more variable running mechanics.

Impact of Strike Pattern on Accuracy

Strike patterns had limited influence on the differences between single- and dual-IMU setups. While forefoot strikers often showed slightly higher dorsi-/plantarflexion errors near toe-off (see Fig. 11) the overall pattern of differences between the two sensor configurations remained consistent across strike patterns.

In early stance, the flat-foot assumption used in the single-IMU estimation appeared to match actual foot posture more often for forefoot strikers, potentially reducing early stance errors. Rearfoot strikers, on the other hand, showed a brief drop in error around 10% of the gait cycle, when the foot transitions from heel contact to full-foot contact and temporarily aligns with the estimation model.

Despite these phase-specific effects, no consistent advantage emerged for either strike pattern. As shown in Tabs. 1 and 2, average errors and correlations varied more between participants than between strike types. While prior work [47] has shown strike-pattern-related differences at the first metatarsophalangeal joint using bone-level imaging, such details will not be fully captured by surface-mounted IMUs. In addition, the forefoot–hindfoot segmentation used here does not isolate the first metatarsophalangeal joint specifically, which may further explain the minimal effect observed in our results.

The Anatomical Division Between Forefoot and Hindfoot

Dividing the foot into forefoot and hindfoot segments is a common simplification in multi-segment foot modelling [22]. However, the foot's true anatomy involves multiple interacting joints that do not conform neatly to such segmentation. Bruening et al. [48] highlight that joint motion in the midfoot often spans multiple segments, meaning the placement of the anatomical boundary can influence calculated joint angles. In the present study, standardized sensor and marker placements were used to reduce variability across participants, ensuring that any anatomical segmentation bias affected both IMU configurations equally.

Practicality of Dual- vs. Single-Sensor Setup

Implementing a dual-IMU setup introduces several practical hurdles, particularly related to forefoot sensor placement. In this study, shoe modifications were required to mount the additional IMU, including cutting holes and altering the shoe structure. This not only increases setup time but can also compromise shoe integrity and introduce variability across trials. Forefoot-mounted sensors are more susceptible to motion artefacts due to twisting and vertical displacement of the soft top part of the shoe during running [49] and tend to show higher variability than more proximal placements [45]. Their proximity to the ground also increases exposure to magnetic disturbances from ferromagnetic objects, such as treadmills, which can raise joint angle RMSE during dynamic movements [50].

Standardizing forefoot IMU placement is another challenge. Existing studies disagree in their recommendations on where and how to attach forefoot sensors [51, 52], complicating reproducibility across labs or clinical settings. By contrast, mounting a single IMU on the hindfoot is more consistent and aligns with standard practices recommended by commercial systems (e.g., Xsens).

Limitations

This study had several methodological limitations that should be considered when interpreting the results. First, the small sample size of six participants restricts the generalizability and statistical power of the outcomes. Although non-parametric tests were used to address non-normal data distributions, the combination of high variability and the small number of conditions per subject likely reduced the ability to detect subtle yet meaningful differences. This concern has also been raised in a meta-analysis on IMU-based gait analysis [42], which identified small sample sizes as a common limitation affecting the strength and reliability of such studies.

Treadmill running also differs from overground gait in terms of mechanics and stride regulation [53], possibly shifting running mechanics during trials. Participants were classified as rearfoot and forefoot strikers during pre-trials on solid ground and without insoles. The combination of treadmill use and pressure insoles, known to introduce foot stiffness and alter foot ankle joint mobility [54], may have introduced unmonitored changes to strike patterns during the actual data collection. This may partially explain why the accuracy differences between strike patterns were not clearly evident.

The study only examined moderate running speeds (9 kph and 11 kph), which limits conclusions about velocity-related effects. However, even within this narrow range, results showed an increase in HF/FF joint angle errors in all planes at the higher speed (Fig. 10), suggesting that faster movement may amplify sensor-related artefacts [14]. Additional testing at higher velocities is needed to better understand how speed influences different IMU sensor configurations.

Regarding the single-IMU setup, the forefoot orientation estimation was implemented as a practical alternative to the closed-source MVN algorithm, which might yield better accuracy, potentially offering a more precise approximation of forefoot orientation. However it was inaccessible due to software restrictions caused by sensor switching in the model. While this limits comparability, previous research suggests that during thw swing, the foot behaves like a rigid segment with minimal internal motion [45], partially supporting the validity of the estimation method used.

CONCLUSION

This study compared single- and dual-IMU foot setups to assess whether adding an extra sensor significantly improves the accuracy of kinematic foot modelling during running. The dual-IMU configuration generally provided smoother and more accurate HF/FF joint angle estimations around critical dynamic phases, the toe-off, compared to the single-sensor setup.

Foot strike pattern (RFS vs. FFS) did not strongly affect the overall accuracy difference between setups, suggesting that the influence of strike type on foot segment modelling is limited in this context. This is consistent with prior work reporting that strike pattern primarily affects ankle joint angles, not other foot joints [31].

Both IMU setups exhibited reduced accuracy at higher running speeds, showing increased variability and errors at 11 kph compared to 9 kph, but without clear superiority of either the single- or dual-sensor configuration. This suggests that at higher velocities, the practical benefits of using a dual-sensor setup to directly measure forefoot motion are less evident, as the increased speed similarly impacts both setups.

The decision to use a dual-IMU setup involves a trade-off between accuracy and practicality. While the dual-IMU setup improved accuracy at toe-off, overall accuracy across the gait cycle was comparable to the single-sensor setup. It also introduced logistical challenges, including more complex sensor placement, shoe modifications, and increased susceptibility to motion and magnetic artefacts. Despite these challenges, the setup may still be justified if the goal is to detect clinically relevant changes. Ultimately, the decision should balance accuracy needs and practical feasibility based on the specific goals of the analysis, as already proposed in walking-based studies [27].

Further work should include larger and more diverse samples, a broader range of running speeds, and overground testing to improve generalizability. Standardized sensor attachment, ideally without shoe modification, would enhance consistency and feasibility in clinical or field use. Future comparisons should also consider commercially available estimation models, such as MVN (Xsens), to evaluate sensor setups using standardized orientation outputs. The single-IMU's assumption of identical forefoot and hindfoot internal/external rotation (heading) could help mitigate the drift and may be useful for stride-by-stride heading correction. Finally, while benefits of multi-segment IMU models have been shown in walking [27, 26], similar validation is still needed for running gait.

REFERENCES

[1] L. C. Hespanhol Junior, J. D. Pillay, W. van Mechelen, and E. Verhagen, Meta-analyses of the effects of habitual running on indices of health in physically inactive adults, *Sports Medicine*, vol. 45, no. 10, pp. 1455–1468, Jul. 2015.

[2] R. N. van Gent, D. Siem, M. van Middelkoop, A. G. van Os, S. M. A. Bierma-Zeinstra, and B. W. Koes, Incidence and determinants of lower extremity running injuries in long distance runners: a systematic review, *British Journal of Sports Medicine*, vol. 41, no. 8, pp. 469–480, Aug. 2007.

[3] S. Willwacher, M. Kurz, J. Robbin, M. Thelen, J. Hamill, L. Kelly, and P. Mai, Running-related biomechanical risk factors for overuse injuries in distance runners: A systematic review considering injury specificity and the potentials for future research, *Sports Medicine*, vol. 52, no. 8, pp. 1863–1877, Aug. 2022.

[4] M. P. van der Worp, D. S. M. ten Haaf, R. van Cingel, A. de Wijer, M. W. G. N. van der Sanden, and J. B. Staal, Injuries in runners; a systematic review on risk factors and sex differences, *PLOS One*, vol. 10, no. 2, e0114937, Feb. 2015.

[5] V. Jakob, A. Küderle, F. Kluge, J. Klucken, B. M. Eskofier, J. Winkler, M. Winterholler, and H. Gassner, Validation of a sensor-based gait analysis system with a gold-standard motion capture system in patients with parkinson's disease, *Sensors*, vol. 21, no. 22, p. 7680, Nov. 2021.

[6] S. Hockett, S. Dunbar, C. Williams, R. Sturdivant, B. Garner, and J. Rylander, Comparison of spatiotemporal gait parameter measurements across various emulated foot strike patterns between the tekscan® strideway™ pressure sensitive walkway and gold-standard marker-based motion capture, *Journal of Biomechanics*, vol. 176, p. 112310, Nov. 2024.

[7] A. Leardini, P. Caravaggi, T. Theologis, and J. Stebbins, Multi-segment foot models and their use in clinical populations, *Gait & Posture*, vol. 69, pp. 50–59, Mar. 2019.

[8] H. J. Yoo, H. S. Park, D. Lee, S. H. Kim, G. Y. Park, T. Cho, and D. Y. Lee, Comparison of the kinematics, repeatability, and reproducibility of five different multi-segment foot models, *Journal of Foot and Ankle Research*, vol. 15, no. 1, Jan. 2022.

[9] R. Mason, L. T. Pearson, G. Barry, F. Young, O. Lennon, A. Godfrey, and S. Stuart, Wearables for running gait analysis: A systematic review, *Sports Medicine*, vol. 53, no. 1, pp. 241–268, Jan. 2023.

[10] P. Picerno, 25 years of lower limb joint kinematics by using inertial and magnetic sensors: A review of methodological approaches, *Gait & Posture*, vol. 51, pp. 239–246, Jan. 2017.

[11] H. Schepers, H. Koopman, and P. Veltink, Ambulatory assessment of ankle and foot dynamics, *IEEE Transactions on Biomedical Engineering*, vol. 54, no. 5, pp. 895–902, May 2007.

[12] P. Picerno, A. Cereatti, and A. Cappozzo, Joint kinematics estimate using wearable inertial and magnetic sensing modules, *Gait & Posture*, vol. 28, no. 4, pp. 588–595, Nov. 2008.

[13] D.-K. Chew, K. J.-H. Ngoh, D. Gouwanda, and A. A. Gopalai, Estimating running spatial and temporal parameters using an inertial sensor, *Sports Engineering*, vol. 21, no. 2, pp. 115–122, Oct. 2018.

[14] Z. Zeng, Y. Liu, X. Hu, M. Tang, and L. Wang, Validity and reliability of inertial measurement units on lower extremity kinematics during running: A systematic review and meta-analysis, *Sports Medicine - Open*, vol. 8, no. 1, p. 86, Jun. 2022.

[15] Y.-C. Lin, K. Price, D. S. Carmichael, N. Maniar, J. T. Hickey, R. G. Timmins, B. C. Heiderscheit, S. S. Blemker, and D. A. Opar, Validity of inertial measurement units to measure lower-limb kinematics and pelvic orientation at submaximal and maximal effort running speeds, *Sensors*, vol. 23, no. 23, p. 9599, Dec. 2023.

[16] S. Park and S. Yoon, Validity evaluation of an inertial measurement unit (imu) in gait analysis using statistical parametric mapping (spm), *Sensors*, vol. 21, no. 11, p. 3667, May 2021.

[17] F. Young, R. Mason, C. Wall, R. Morris, S. Stuart, and A. Godfrey, Examination of a foot mounted imu-based methodology for a running gait assessment, *Frontiers in Sports and Active Living*, vol. 4, Sep. 2022.

[18] B. L. Scheltinga, H. Usta, J. Reenalda, and J. H. Buurke, Estimating vertical ground reaction force during running with 3 inertial measurement units, *Journal of Biomedical Engineering and Biosciences*, vol. 9, pp. 31–38, Nov. 2022.

[19] M. Falbriard, F. Meyer, B. Mariani, G. P. Millet, and K. Aminian, Accurate estimation of running temporal parameters using foot-worn inertial sensors, *Frontiers in Physiology*, vol. 9, Jun. 2018.

[20] J. C. Wager and J. H. Challis, Mechanics of the foot and ankle joints during running using a multi-segment foot model compared with a single-segment model, *PLOS One*, vol. 19, no. 2, e0294691, Feb. 2024.

[21] Y. Matsumoto, N. Ogihara, H. Hanawa, T. Kokubun, and N. Kanemura, Novel multi-segment foot model incorporating plantar aponeurosis for detailed kinematic and kinetic analyses of the foot with application to gait studies, *Frontiers in Bioengineering and Biotechnology*, vol. 10, Jun. 2022.

[22] A. Leardini, M. Benedetti, L. Berti, D. Bettinelli, R. Nativo, and S. Giannini, Rear-foot, mid-foot and fore-foot motion during the stance phase of gait, *Gait & Posture*, vol. 25, no. 3, pp. 453–462, Mar. 2007.

[23] M. Carson, M. Harrington, N. Thompson, J. O'Connor, and T. Theologis, Kinematic analysis of a multi-segment foot model for research and clinical applications: a repeatability analysis, *Journal of Biomechanics*, vol. 34, no. 10, pp. 1299–1307, Oct. 2001.

[24] D. Winter, *Biomechanics and Motor Control of Human Movement*. Wiley, 2009. [Online]. Available: https://books.google.nl/books?id=_bFHL08IWfwC

[25] F. Camargo-Junior, M. Ackermann, J. F. Loss, and I. C. Sacco, Influence of center of pressure estimation errors on 3d inverse dynamics solutions during gait at different velocities, *Journal of Applied Biomechanics*, vol. 29, no. 6, pp. 790–797, Dec. 2013.

[26] H. Rouhani, J. Favre, X. Crevoisier, and K. Aminian, Measurement of multi-segment foot joint angles during gait using a wearable system, *Journal of Biomechanical Engineering*, vol. 134, no. 6, Jun. 2012.

[27] N. Okkalidis, G. Marinakis, A. Gatt, M. K. Bugeja, K. P. Camilleri, and O. Falzon, A multi-segment modelling approach for foot trajectory estimation using inertial sensors, *Gait & Posture*, vol. 75, pp. 22–27, Jan. 2020.

[28] L. Bauer, M. A. Hamberger, W. Böcker, H. Polzer, and S. F. Baumbach, Reliability testing of an imu-based 2-segment foot model for clinical gait analysis, *Gait & Posture*, vol. 114, pp. 112–118, Oct. 2024.

[29] L. Bauer, M. A. Hamberger, W. Böcker, H. Polzer, and S. F. Baumbach, Development of an imu based 2-segment foot model for an applicable medical gait analysis, *BMC Musculoskeletal Disorders*, vol. 25, no. 1, p. 606, Jul. 2024.

[30] B. H. Kim, S. H. Hong, I. W. Oh, Y. W. Lee, I. H. Kee, and S. Y. Lee, Measurement of ankle joint movements using imus during running, *Sensors*, vol. 21, no. 12, p. 4240, Jun. 2021.

[31] A. B. Matias, P. Caravaggi, U. T. Taddei, A. Leardini, and I. C. N. Sacco, Rearfoot, midfoot, and forefoot motion in naturally forefoot and rearfoot strike runners during treadmill running, *Applied Sciences*, vol. 10, no. 21, p. 7811, Nov. 2020.

[32] Z. Zeng, Y. Liu, P. Li, and L. Wang, Validity and reliability of inertial measurement units measurements for running kinematics in different foot strike pattern runners, *Frontiers in Bioengineering and Biotechnology*, vol. 10, Dec. 2022.

[33] A. Estep, S. Morrison, S. Caswell, J. Ambegaonkar, and N. Cortes, Differences in pattern of variability for lower extremity kinematics between walking and running, *Gait & Posture*, vol. 60, pp. 111–115, Feb. 2018.

[34] D. G. E. Robertson, G. E. Caldwell, J. Hamill, G. Kamen, and S. N. Whittlesey, *Research Methods in Biomechanics*. Human Kinetics, 2014.

[35] D. Roetenberg, H. Luinge, and P. Slycke, Xsens mvn: Full 6dof human motion tracking using miniature inertial sensors, *Xsens Motion Technol. BV Tech. Rep.*, vol. 3, 01 2009.

[36] R. E. Fellin, W. C. Rose, T. D. Royer, and I. S. Davis, Comparison of methods for kinematic identification of footstrike and toe-off during overground and treadmill running., *Journal of science and medicine in sport*, vol. 13, no. 6, pp. 646–650, Nov. 2010.

[37] Z. Zeng, Y. Liu, and L. Wang, Validity of imu measurements on running kinematics in non-rearfoot strike runners across different speeds, *Journal of Sports Sciences*, vol. 41, no. 11, pp. 1083–1092, Jun. 2023.

[38] R. Taylor, Interpretation of the correlation coefficient: A basic review, *Journal of Diagnostic Medical Sonography*, vol. 6, no. 1, pp. 35–39, Jan. 1990.

[39] W. Schallig, J. C. van den Noort, J. McCahill, J. Stebbins, A. Leardini, M. Maas, J. Harlaar, and M. M. van der Krogt, Comparing the kinematic output of the oxford and rizzoli foot models during normal gait and voluntary pathological gait in healthy adults, *Gait & Posture*, vol. 82, pp. 126–132, Oct. 2020.

[40] R. Wang, C. K. Thur, E. M. Gutierrez-Farewik, P. Wretenberg, and E. Broström, One year follow-up after operative ankle fractures: A prospective gait analysis study with a multi-segment foot model, *Gait & Posture*, vol. 31, no. 2, pp. 234–240, Feb. 2010.

[41] P. Levinger, G. S. Murley, C. J. Barton, M. P. Cotchett, S. R. McSweeney, and H. B. Menz, A comparison of foot kinematics in people with normal- and flat-arched feet using the oxford foot model, *Gait & Posture*, vol. 32, no. 4, pp. 519–523, Oct. 2010.

[42] D. Kobsar, J. M. Charlton, C. T. Tse, J.-F. Esculier, A. Graffos, N. M. Krowchuk, D. Thatcher, and M. A. Hunt, Validity and reliability of wearable inertial sensors in healthy adult walking: a systematic review and meta-analysis, *Journal of NeuroEngineering and Rehabilitation*, vol. 17, no. 1, p. 62, May 2020.

[43] D. Debertin, A. Wargel, and M. Mohr, Reliability of xsens imu-based lower extremity joint angles during in-field running, *Sensors*, vol. 24, no. 3, p. 871, Jan. 2024.

[44] J.-T. Zhang, A. C. Novak, B. Brouwer, and Q. Li, Concurrent validation of xsens mvn measurement of lower limb joint angular kinematics, *Physiological Measurement*, vol. 34, no. 8, pp. 63–69, Aug. 2013.

[45] M. Zrenner, A. Küderle, N. Roth, U. Jensen, B. Dümler, and B. M. Eskofier, Does the position of foot-mounted imu sensors influence the accuracy of spatio-temporal parameters in endurance running?, *Sensors*, vol. 20, no. 19, p. 5705, Oct. 2020.

[46] G. Patel, R. Mullerpatan, B. Agarwal, T. Shetty, R. Ojha, J. Shaikh-Mohammed, and S. Sujatha, Validation of wearable inertial sensor-based gait analysis system for measurement of spatiotemporal parameters

and lower extremity joint kinematics in sagittal plane, *Proceedings of the Institution of Mechanical Engineers, Part H: Journal of Engineering in Medicine*, vol. 236, no. 5, pp. 686–696, May 2022.

[47] K. Wu, X. Sun, D. Ye, F. Zhang, S. Zhang, and W. Fu, Effects of different habitual foot strike patterns on in vivo kinematics of the first metatarsophalangeal joint during shod running—a statistical parametric mapping study, *Frontiers in Bioengineering and Biotechnology*, vol. 11, Sep. 2023.

[48] D. A. Bruening, K. M. Cooney, and F. L. Buczek, Analysis of a kinetic multi-segment foot model part ii: Kinetics and clinical implications, *Gait & Posture*, vol. 35, no. 4, pp. 535–540, 4 2012.

[49] J. Sinclair, P. Taylor, J. Hebron, and N. Chockalingam, Differences in multi-segment foot kinematics measured using skin and shoe mounted markers, *The Foot and Ankle Online Journal*, vol. 7, Jun. 2014.

[50] X. Robert-Lachaine, H. Mecheri, C. Larue, and A. Plamondon, Effect of local magnetic field disturbances on inertial measurement units accuracy, *Applied Ergonomics*, vol. 63, pp. 123–132, Sep. 2017.

[51] A. Küderle, N. Roth, J. Zlatanovic, M. Zrenner, B. Eskofier, and F. Kluge, The placement of foot-mounted imu sensors does affect the accuracy of spatial parameters during regular walking, *PLOS One*, vol. 17, e0269567, Jun. 2022.

[52] A. R. Anwary, H. Yu, and M. Vassallo, Optimal foot location for placing wearable imu sensors and automatic feature extraction for gait analysis, *IEEE Sensors Journal*, vol. 18, no. 6, pp. 2555–2567, Mar. 2018.

[53] I. V. Caekenberghe, V. Segers, P. Willems, T. Gosseye, P. Aerts, and D. D. Clercq, Mechanics of overground accelerated running vs. running on an accelerated treadmill, *Gait & Posture*, vol. 38, no. 1, pp. 125–131, May 2013.

[54] L. Jin, The influence of different footwear insole stiffness on center of pressure and ankle kinematics during walking: A case report, *Biomechanics*, vol. 2, no. 2, pp. 205–212, May 2022.

DECLARATION OF AI USE

During the preparation of this work, the author used ChatGPT (OpenAI) in order to support the generation and organization of ideas, creation of the thesis outline and structure, refinement of grammar and wording, assistance with writing and debugging MATLAB code, and support with LaTeX formatting. Additionally, Grammarly was used to assist with grammar and spelling corrections, including AI-based suggestions.

After using this tool, the author reviewed and edited the content as needed and takes full responsibility for the content of the work.